Materials Science and Engineering A 528 (2011) 3330–3336

Contents lists available at ScienceDirect

Materials Science and Engineering A

journal homepage: www.elsevier.com/locate/msea

Influence of composition on mechanical behaviour of porcelain tile. Part III: Effect of the cooling rate of the firing cycle☆

Agenor De Noni Junior[a,b,*], Dachamir Hotza[b], Vicente Cantavella Soler[c], Enrique Sánchez Vilches[c]

[a] Instituto Maximiliano Gaidzinski (IMG), Rua Dr. Edson Gaidzinski, 352, 88845-000 Cocal do Sul, Santa Catarina, Brazil
[b] Universidade Federal de Santa Catarina (UFSC), Campus Universitário Trindade, 88040-900 Florianópolis, Brazil
[c] Instituto de Tecnologia Cerámica (ITC), Campus Universitario Riu Sec, 12006 Castellón, Spain

ARTICLE INFO

Article history:
Received 22 September 2010
Received in revised form
22 December 2010
Accepted 22 December 2010
Available online 7 January 2011

Keywords:
Porcelain tile
Firing
Cooling rate
Mechanical properties
Residual stresses

ABSTRACT

This paper is the third part of a study focusing on determining the influence of the porcelain tile composition on mechanical behaviour of sintered bodies. Tile compositions were prepared according to a simplex-centroid mixture design set out in Part I of this research, in which the microstructural characterisation of sintered specimens was carried out. In Part II the influence of the starting composition on the mechanical properties of sintered porcelain tile was evaluated on the basis of the linear elastic fracture mechanics. Finally, in this last Part, ceramic bodies from seven compositions were subjected to fast cooling after firing, in order to reproduce the industrial cooling rates. The main objective was to analyze the influence of the mineralogical composition of the starting mixture on the development of macroscopic residual stress and growth of flaw size. When the pieces were subjected to fast cooling, flaw size was the main factor determining the variation of the mechanical strength. This increase in flaw size can be interpreted from the Weibull modulus, from 6 to 8 in those mixtures, with high deterioration of mechanical properties. The mullite hypothesis as a strengthening mechanism in triaxial porcelains was clearly manifested when the samples are fast cooled. This mechanism was the main responsible for the strengthening, what contrasts with the increase in flaw size. The microscopic residual stress caused by the thermal expansion mismatch of the phases also acted as a reinforcement mechanism.

1. Introduction

Porcelain tile is a large scale product subjected to heat treatment at temperatures between 1180 and 1220 °C with cold-to-cold times from 40 to 60 min. The maximum firing temperature is normally determined by maximum densification. The cooling stage is done as fast as possible up to 650 °C. Between 650 and 500 °C, which corresponds to the allotropic transformation zone of quartz (573 °C), the cooling rate is reduced to prevent rupture of the product, and then increased again up to environment temperature [1,2].

The first part of industrial cooling corresponds to the range between the fluxes melting temperature and the glass transition temperature of the vitreous phase (T_g). As described in previous publications [3,4], porcelain tiles that experience fast cooling in this stage develop a macroscopic residual stresses profile. For typical tempering of glasses, which are more homogeneous materials than porcelain tiles, Eq. (1) represents an estimation of the maximum residual stress developed at the surface [5], σ_s.

$$\sigma_s = -\frac{\alpha \cdot E \cdot h^2 \cdot \nu}{12 \cdot (1-\upsilon) \cdot k} \quad (1)$$

where α is the thermal expansion coefficient in the rigid state; E is the Young's modulus; h is the thickness; ν is the cooling rate; υ is the Poisson's module; $k$is the thermal diffusivity.

Since at the surface a compressive stress is developed, an increase in mechanical strength of the final product is expected. However, an important difference, when compared to the traditional tempered glass, is the presence of quartz particles in porcelain tile. In this case, peripheral cracks around particle–matrix interfaces are formed as a consequence of microscopic residual stresses [6]. During fast cooling, thermal stresses take place on the surface. Therefore, after the quartz allotropic transformation, a subcritical growth of peripheral cracks starts, which may lead to

☆ Based in part on the thesis submitted by A. De Noni Jr. for the Ph.D. degree in Materials Science and Engineering (PGMAT), Universidade Federal de Santa Catarina (UFSC), Brazil, 2007. This work was financially supported by the Brazilian Research Agency CAPES, under scholarship 2933-05-5 and co-financed by the Spanish Ministry of Industry, Tourism, and Trade for the Technology Institute Support Programme, under Grant FIT-030000-2005-315/FIT-030000-2006-119.

* Corresponding author at: Instituto Maximiliano Gaidzinski (IMG), Rua Dr. Edson Gaidzinski, 352, 88845-000 Cocal do Sul, Santa Catarina, Brazil.
Tel.: +55 48 3447 7736; fax: +55 48 3447 7736.
E-mail addresses: agenordenoni@imgnet.org.br, agenordenoni@gmail.com (A. De Noni Junior), hotza@enq.ufsc.br (D. Hotza), vicente.cantavella@itc.uji.es (V. Cantavella Soler), enrique.sanchez@itc.uji.es (E. Sánchez Vilches).

0921-5093/$ – see front matter © 2011 Elsevier B.V. All rights reserved.
doi:10.1016/j.msea.2010.12.086

Table 1
Mineralogical composition of the sintered composition (volume fraction).

Composition	M + KG	Q	A + AG
C1	0.17	0.40	0.43
C2	0.44	0.10	0.45
C3	0.17	0.10	0.73
C4	0.30	0.25	0.44
C5	0.17	0.25	0.58
C6	0.30	0.10	0.60
C7	0.26	0.20	0.54

a material deterioration through increasing of Griffith flaw size. A previous paper [4] has shown that Eq. (2) can describe the mechanical strength of a material with macroscopic residual stress profile:

$$\sigma_{ta} = \frac{K_{IC}}{Y \cdot a^{1/2}} - \sigma_s \cdot \left(\frac{2 \cdot h}{\pi} \cdot a + 1\right) \quad (2)$$

where K_{IC} is the material fracture toughness without macroscopic residual stress; $a$is the Griffith flaw size; $Y$is the calibration factor of fracture mechanics (1.98 in this case [4,7]).

In previous papers [3,4], it became clear that the fastest growing natural defect size occurs with (i) increasing cooling rate, (ii) increasing particle size of quartz and (iii) reducing the fracture energy of the material. Those studies were conducted with an industrial composition of a porcelain tile from a spray-dried powder.

This research has been conducted to study the mechanical properties of seven compositions of porcelain tile, described in Parts I and II of this paper, [8,9] subjected to fast cooling after firing, trying to reproduce the industrial cooling rates. Those seven compositions were formulated from a kaolin–quartz–feldspar system using a simplex-centroid mixture design described previously [8]. The main objective here is to analyze the influence of the mineralogical composition of the starting mixture on the development of macroscopic residual stress and the growth of flaw size on porcelain tile fired bodies.

2. Experimental procedure

The seven compositions used in this paper have been characterized in previous papers [8,9]. Table 1 shows the mineralogical composition of the sintered compositions based on the volume fraction of components grouped according to their microstructural distribution, as previously described [8]: (a) M + KG, corresponds to mullite and kaolinite glass (b) Q, to quartz, quartz addition (c) A + AG, to residual albite and albite glass. The industrial formulations are close to the C7 mix. The remaining compositions cover the wide range generally practiced in the industry. However, quartz is rarely added as a pure raw material, but it is rather associated to clay and feldspar minerals. Kaolinite is not the unique clay mineral phase; normally illite and montmorillonite are also present in order to increase green strength and reduce firing temperature, generating more glass phase than pure kaolinite.

In order to plot the results using a triaxial diagram, the mass fraction of each component (X_i) were converted into a pseudo-component (pX_i) according to Eq. (3).

$$pX_i = \frac{X_i - L_{li}}{L_{ui} - L_{li}} \quad (3)$$

where L_{ui} and L_{li} are the upper and lower limits for component i, respectively.

The specimens were prepared according to laboratory procedures in order to simulate industrial processing conditions [8]. Fig. 1 shows the assembly used to reproduce fast cooling. After the holding time at maximum firing temperature (between 1220 and 1260 °C), the refractory plate with 8 specimens (P1) was removed from the kiln, resting on a refractory support (P2) and cooled using fans (P3) and compressed air (P4) down to 650 °C at a cooling rate of ~9.5 °C/s. The cooling below 650 °C was conducted with ventilation system turned off and the pieces were isolated to reduce the cooling rate during the allotropic transformation of quartz (~3.6 °C/s). The specimens remained apart until the room temperature was reached. This procedure has been already described in previous papers [3,4].

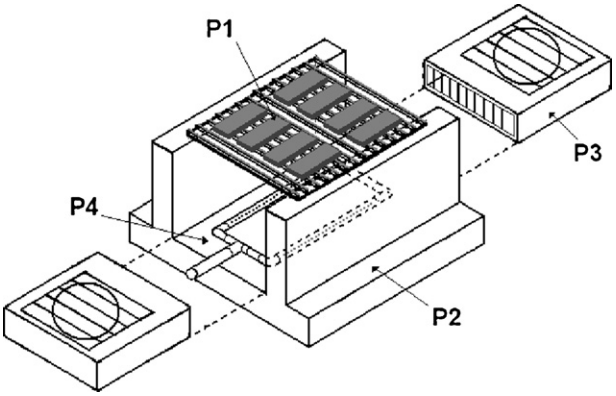

Fig. 1. Device designed for fast cooling the specimens outside the kiln, comprised by a refractory plate (P1), a refractory support (P2), two side fans (P3) and a compressed air diffuser (P4).

Three-point bending strength tests were performed with 12 pieces for each mixture, using a universal testing machine (Instron 6027). The macroscopic residual stresses were measured with one specimen of each mixture by the deformation–relaxation method with incremental cuts [10], using a 0.4-mm-thick diamond cutting disc and rectangular strain gauges with a 3-mm-long grid (HBM). The values of elastic modulus and fracture toughness were obtained from the same mixtures, but subjected to slow cooling [9]. Flaw size was determined from Eq. (2).

Linear thermal expansion curves between 625 and 750 °C were measured with two specimens of each mixture by contact dilatometry (Netzsch DIL 402C) with a heating rate of 10 °C/min. Microscopic residual stress on quartz particles was evaluated by X-ray diffraction from displacement of diffraction peaks for both [1 1 2] and [2 1 1] planes of quartz [6]. The experiments were carried out by a diffractometer (Broker AXS D8, Germany) with Cu K ($\alpha 1 + \alpha 2$) radiation, reading time of 0.01°/s in the 2θ range of 10–70° using an internal corundum standard (1976-NIST, USA). The mathematical treatment of the diffraction data to obtain the value of microscopic residual stress was detailed in a previous paper [6].

3. Results and discussion

3.1. Macroscopic residual stresses on surface

Table 2 contains data from macroscopic residual stresses on the surface and the parameters that determine the residual stresses,

Table 2
Macroscopic residual stress on the surface (σ_s), linear thermal expansion coefficient ($\alpha_{625-700}$) and Young's modulus (E) of prepared mixtures.

Mixture	σ_s (MPa)	$\alpha_{625-750} \times 10^{-7}$ (°C^{-1})	E (GPa)
C1	−18	36	50
C2	−33	48	60
C3	−34	62	53
C4	−20	44	56
C5	−24	48	51
C6	−34	54	57
C7	−24	47	55

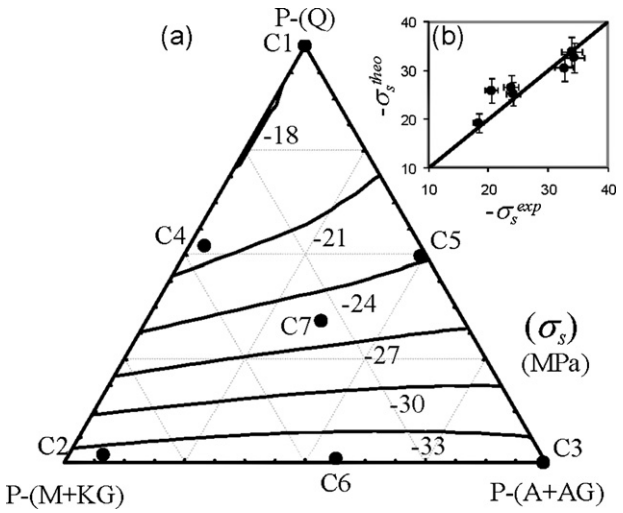

Fig. 2. (a) Macroscopic residual stress (σ_s) on the surface as a function of the mineralogical composition, (b) comparison between experimental (σ_s^{exp}) and theoretical values (σ_s^{theo}), according to Eq. (1).

according to Eq. (1). The cooling rate ($v = 9.5\,^{\circ}C/s$) and the thickness of specimens ($h = 7.00$ mm) remained constant. The thermal diffusivity, for simplification, has been considered constant and equal to that of industrial porcelain [4] ($k = (3.4 \pm 0.2) \times 10^{-7}$ m^2/s).

Fig. 2a represents the macroscopic residual stress on the surface as a function of mineralogical composition of the sintered parts. The compositions with lower content of quartz have developed the highest levels of residual stresses. The Cartesian graph, Fig. 2b, shows the experimental value of residual stresses in comparison with the value estimated by Eq. (1) and bisecting the line. The development of macroscopic residual stresses can be adequately described according to a glass tempering process. The average error was 5%, as described by the authors in previous papers [3,4]. Finally, the mixtures with higher content of quartz present both a lower thermal expansion and a lower Young's modulus, leading to decreasing residual stresses.

The fact that mixtures with higher content of quartz resulted in a lower coefficient of thermal expansion confirms that between 625 and 750 °C the quartz present in the samples is β-quartz, which has a coefficient of thermal expansion $\alpha_{\beta\text{-}Q} \sim 0\,^{\circ}C^{-1}$. The other system components, M + KG and A + AG, respectively, represent the thermal expansion coefficients of $\alpha_{M+KG(625-750)} \sim 32 \times 10^{-7}\,^{\circ}C^{-1}$ and $\alpha_{A+AG(625-750)} \sim 74 \times 10^{-7}\,^{\circ}C^{-1}$. Fig. 3 shows the relationship between the results of the measured thermal expansion coefficient compared to the theoretically estimated values, being the

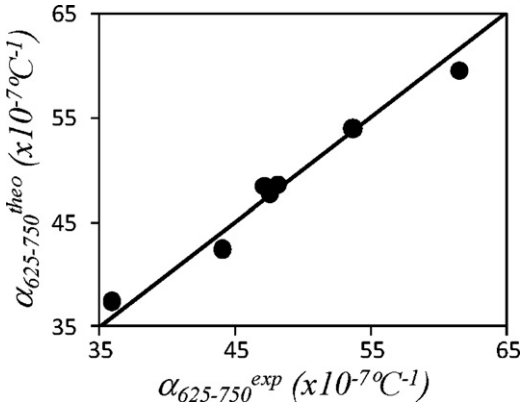

Fig. 3. Comparison between experimental ($\alpha^{exp}_{625\text{-}750}$) and theoretical ($\alpha^{theo}_{625\text{-}750}$) values of coefficient of thermal expansion for the studied mixtures.

Table 3
Mechanical properties of the mixture according to Eq. (2) (fast cooling); difference between mechanical strength and flaw size from specimens subjected to slow cooling (part II [9]), $\Delta\sigma_{ta\text{-}f}$ and Δa respectively.

Mixture	σ_{ta} (MPa)	$\Delta\sigma_{ta\text{-}f}$ (MPa)	K_{IC} (MPa m$^{1/2}$)	a (μm)	Δa (μm)	Wm[a]
C1	78.3	5.2	1.74	201	55	8
C2	73.9	12.2	1.38	235	107	7
C3	71.8	9.9	1.68	361	174	6
C4	90.8	20.7	1.59	125	-6	30
C5	72.2	-0.7	1.72	280	138	8
C6	84.3	17.6	1.53	205	71	18
C7	87.5	17.1	1.62	154	19	27

[a] Wm—Weibull's modulus.

average error 3%. The additive behaviour of this property was confirmed.

3.2. Mechanical properties

Table 3 lists the data for the parameters of Eq. (2) (σ_{ta}, K_{IC}, a) together with values of Weibull's modulus (Wm). In addition, we have also included values of the increase in mechanical strength, $\Delta\sigma_{ta\text{-}f}$, and the flaw size, Δa, in relation to those specimens subjected to slow cooling published in a previous paper [4]. It is noticed that in almost all mixtures there was a significant increase in mechanical strength associated to tempering. However, flaw size also increased, which partially mitigated the effect of tempering. There are two extreme cases: (1) mixture C5, where there was no increase in mechanical strength, and (2) mixture C4, in which there was no increase in the size of the natural defect and where the highest increase in compressive strength was developed. These two cases will be discussed later.

3.3. Analysis of mechanical strength as a function of mineralogical composition

Taking as a reference the mechanical strength of mixture C7, σ_{ta7}, the difference between the mechanical strength of any mixture, σ_{taj}, with respect to C7 can be written as a Taylor series expansion of Eq. (2), expressed in terms of K_{IC}, σ_s and a as follows:

$$\Delta\sigma_{taj} = \Delta K_{ICj} \cdot \left.\frac{\partial\sigma_{ta}}{\partial K_{IC}}\right|_{\bar{K}_{ICj},\bar{\sigma}_{sj},\bar{a}_j} + \Delta\sigma_{sj} \cdot \left.\frac{\partial\sigma_{ta}}{\partial\sigma_s}\right|_{\bar{K}_{ICj},\bar{\sigma}_{sj},\bar{a}_j} + \Delta a_j \cdot \left.\frac{\partial\sigma_{ta}}{\partial a}\right|_{\bar{K}_{ICj},\bar{\sigma}_{sj},\bar{a}_j} \quad (4)$$

$$\Delta\sigma_{taj}, \Delta K_{ICj}, \Delta\sigma_{sj}, \Delta a_j = \Delta X_j = X_j - X_7 \quad (5)$$

$$\bar{K}_{ICj}, \bar{\sigma}_{sj}, \bar{a}_j = \bar{X}_j = \frac{X_j + X_7}{2} \quad (6)$$

$$\delta X_j = \Delta X_j \frac{\partial\sigma_{ta}}{\partial X} \quad (7)$$

where j is a mixture number; $j = 1$ means mixture C1, for instance.

Each term of Eq. (4) (δK_{ICj}, $\delta\sigma_{sj}$ and δa_j) represents the contribution of the respective property on the variation of mechanical strength for a given mixture related to reference value (C7). Fig. 4 shows the variation of $\Delta\sigma_{taj}$ and δX_j as a function of composition. Negative values mean that, for a given composition, that factor acts to reduce the mechanical strength in respect to the reference composition. The trends presented in the graphs suggest that flaw size is the main factor responsible for mechanical strength changes as a function of mineralogical composition. However, δK_{ICj}, $\delta\sigma_{sj}$, in this case, diminished the deleterious effect of flaw size on mechani-

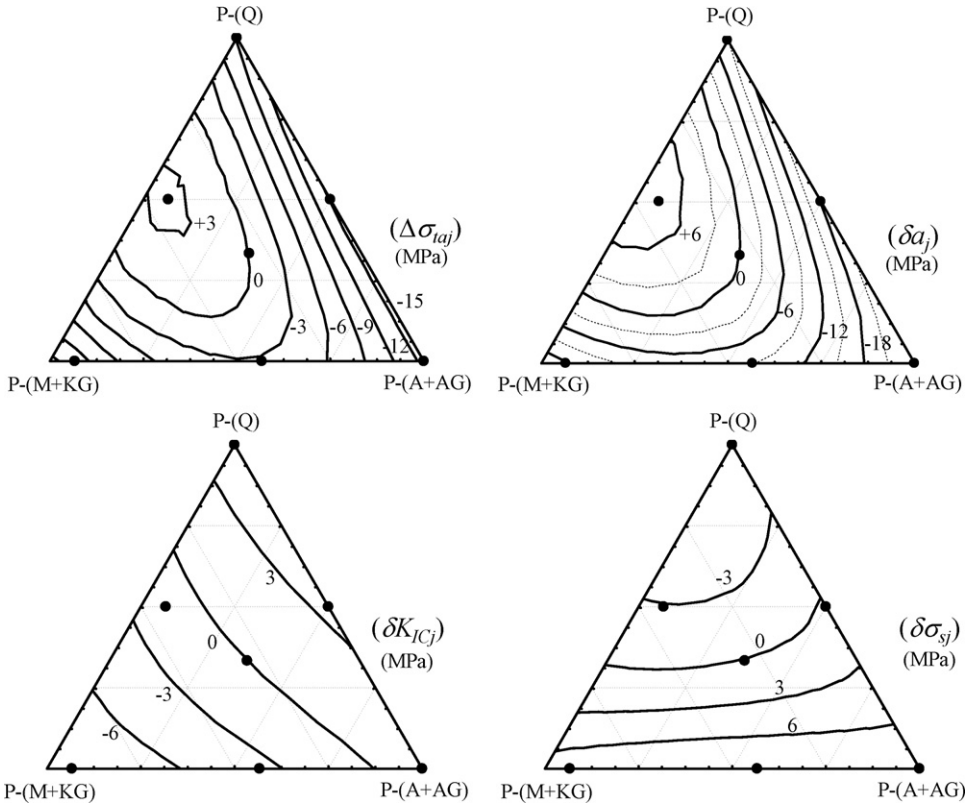

Fig. 4. $\Delta\sigma_{taj}$, δK_{ICj}, $\delta\sigma_{sj}$ and δa_j as a function of mineralogical composition.

cal strength, once the range of $\Delta\sigma_{taj}$ was 19 MPa, δa_j 32 MPa, δK_{ICj} 13 MPa and $\delta\sigma_{sj}$ 14 MPa, respectively.

3.4. Analysis of flaw size increasing

3.4.1. Effect of the mineralogical composition

As described in a previous paper [9], the flaw size did not present a significant correlation with mineralogical composition when the specimens are subjected to slow cooling and did not control the role of mechanical strength. However, for a fast cooling rate, the increasing on flaw size depends on mineralogical composition, which controls the behaviour of mechanical strength. Fig. 5 shows clearly the similarity between mechanical strength (σ_{ta}) and flaw size increasing (Δa) as a function of mineralogical composition. It may be also observed that the region of maximum mechanical strength and minimal flaw size is represented by the C4 mixture, followed by C7 and C6.

The Weibull's modulus (Wm) is related to the extent of the distribution function of flaw size [11]. In a previous paper [12] it was reported that with increasing flaw sizes in specimens subjected to fast cooling, the broader is the dispersion in size of defects, the lower are the Wm values. Fig. 6 shows the variation of Wm as a function of the mineralogical composition, in which the same trend is observed. To $\Delta a > 55$ μm (except for mixture C6), Wm significantly decreases down to 8.

The observed decrease on Weibull's can be attributed to larger flaw sizes for some of the mixture specimens. Table 4 lists the maximum and minimum values of mechanical strength and flaw size for all mixtures. It is noticed that the highest values of mechanical strength had virtually no significant changes as a function of mineralogical composition. However, the lowest values strongly changed. In respect to the maximum flaw size it is observed that mixtures C4, C6 and C7 presented values between 150 and 270 μm, while the blends C1, C2 and C5 presented values between 440 and

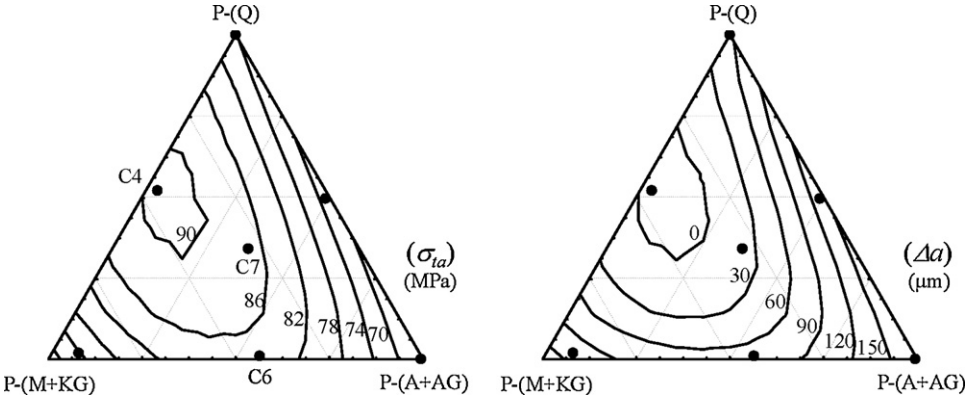

Fig. 5. (a) Mechanical strength (σ_{ta}) and (b) flaw size increasing (Δa) as a function of mineralogical composition.

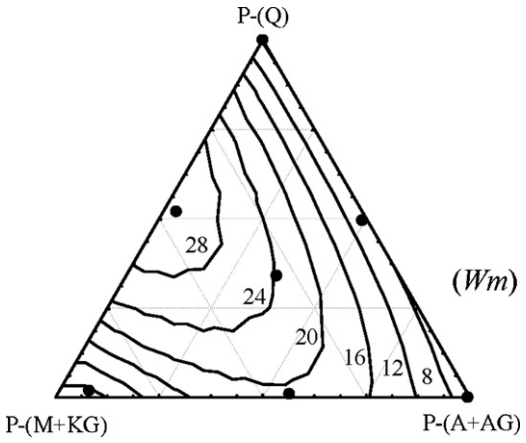

Fig. 6. Weibull's modulus (Wm) as a function on mineralogical composition.

Table 4
Maximum and minimum values of mechanical strength (σ_{ta}) and flaw size (a) for all mixtures.

	σ_{ta}^{max} (MPa)	σ_{ta}^{min} (MPa)	a^{min} (μm)	a^{max} (μm)
C1	91.0	55.9	140	437
C2	89.9	52.0	136	562
C3	89.6	49.0	202	801
C4	94.9	85.6	112	144
C5	86.5	57.5	179	476
C6	92.2	76.4	160	267
C7	92.7	82.7	134	178

560 μm. Mixture C3 shows a maximum value of ~800 μm, which is very high when compared to the minimum value of the same mixture.

For C3 mixture, it was unexpectedly observed that around 20% of the specimens prepared by fast cooling were broken spontaneously after more than 24 h outside of the kiln. Probably for these particular cases, natural flaw sizes were even higher than 800 μm, so that, together with the presence of macroscopic residual stresses, favourable conditions for the fracture were reached. Fig. 7 shows a photograph of one of the broken pieces. In addition to the total rupture (F1), there are areas where the fracture has not collapsed the specimens but reached a large extension (F2 and F3). Those areas are concentrated mainly in sites in which there were no support points in refractory plate and therefore they received more air flow during cooling.

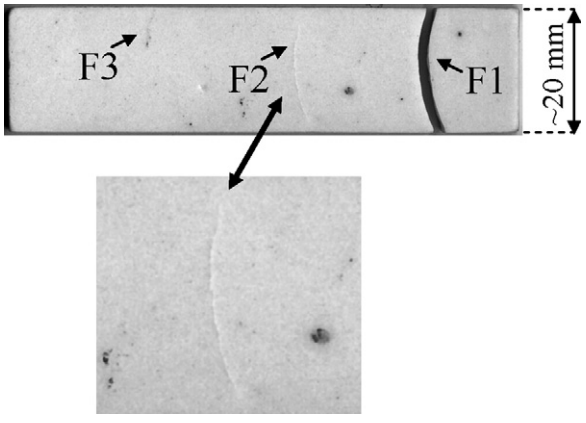

Fig. 7. Photograph of one specimen from mixture C3 that was spontaneously broken after 24 h outside of kiln. Total rupture (F1) and macroscopic cracks (F2, F3).

3.4.2. Mechanism of flaw size growth

In previous papers [3,4,12] it became clear that the increasing in flaw size for specimens subjected to fast cooling is favoured by three factors: (i) the presence of peripheral cracks around the quartz particles, mainly the larger particles, (ii) the presence of tensile thermal stresses on the surface, which increase as the cooling rate gets higher, and (iii) the fracture energy of the material, i.e., lower fracture energy conducts to higher increasing of flaw size.

In the present investigation the quartz particles size did not change, so that for all blends the primary detachments occur at the same temperature. The cooling rate was kept constant. In this way, the differences in thermal stresses, which manifest themselves after the allotropic transformation of quartz, are due only to differences in thermal expansion coefficients and Young's modulus of the mixtures. The fracture energy changes with the composition because of the microscopic residual stresses and the effect of particle dispersion [9].

The experimental procedure conducted during cooling consisted in leading samples from ~650 °C down to room temperature. The thermal gradients were significantly reduced as the pieces cooled down. For this reason, it is expected that the process that increases the flaw size is much more intense at higher temperatures, between 573 and 500 °C, once the contribution of thermal stresses is higher in this range of temperature than for temperatures below 500 °C.

The results of Δa presented in Fig. 4 may be analyzed comparing the mixtures C4, C6 and C7 to mixtures C1, C5 and C3. The first group has lower fracture energy than the second one [9]; however, increased flaw size was more pronounced in C1, C5 and C3. Thus, the mechanisms of enhancing fracture energy observed for slowly cooled specimens (microscopic residual stress and dispersion of crystals of albite) have not been able to prevent microstructural damage of those specimens subjected to fast cooling. The lower thermal stress expected for the mixture C2 has not been able to prevent the increase in the flaw size; this mixture then presented the lowest fracture energy.

The factor that justifies those results is related to the interconnection of mullite crystals [8,9]. For mixtures C4, C6 and C7 the crystals created a continuous network, which probably has prevented the growth of flaw size. For the blends C1, C5 and C3 the mullite is not interconnected. Both mullite crystals and kaolinite glass decrease the fracture energy of the material, subjecting the matrix to microscopic residual tensile stress. This effect is not pronounced at high temperatures and has not been higher than the reinforcement associated to the mullite crystals network. The microscopic compressive stress caused by quartz particles is more intense, being already present even at high temperatures, which also justifies the observed differences between mixtures: Δa for C4 < C7 < C6 and C1 < C5 < C6. For mixture C2, the low amount of quartz added to the excess of M + KG probably has resulted in a much more stressed matrix, and the high temperature has overcome the effect of the interconnection of mullite crystals.

Fig. 8 shows the micrographs of mixtures C2, C4, C5 and C7. All components of the material are indicated in the micrograph of the mixture C7, including the porosity P. It is clear that for the mixture C5, there is no interconnection of mullite crystals. The same was observed for C1 and C3 mixtures [8]. From the composition C7 there is a more pronounced interconnection, which is intensified for C4 and C6 mixtures [8]. For C2 there is an oversupply of interconnected mullite, but that has not hindered the growth of natural defect.

3.5. Analysis of microscopic residual stresses on quartz particles

The presence of peripheral cracks around the quartz particles contribute to the increasing of flaw size. This process occurs mainly from largest quartz particles (about 45 μm [6,12]), since

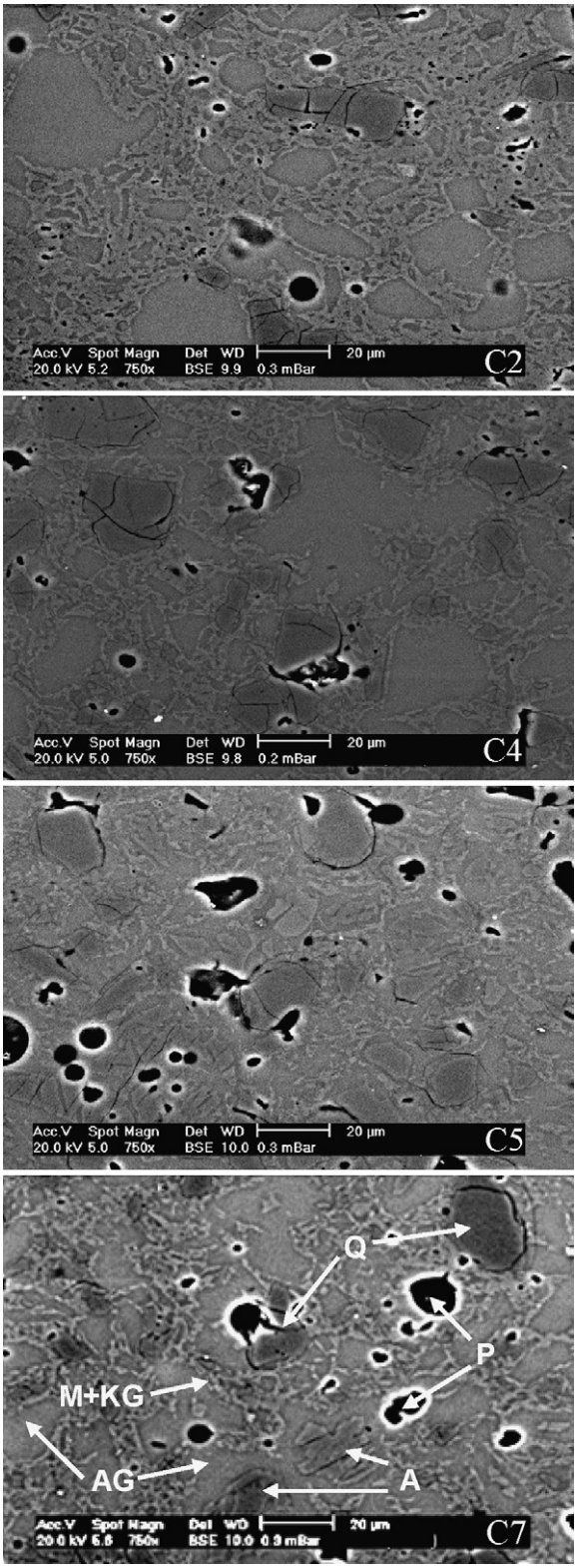

Fig. 8. Micrographs of mixtures C2, C4, C5 and C7. Quartz particles (Q), pores (P), albite particles (A), albite glass (AG), mullite (M) kaolinite glass (KG).

they are the first ones to detach from the matrix. Microscopic residual stresses on quartz particles can be measured for all particles, regardless of their diameter and a priori it should not change for those pieces which were fast cooled [3]. Fig. 9 shows the difference between microscopic residual stress on the quartz particles between the pieces which were slow [9] and fast cooled, respectively. Negative values indicate that microscopic residual stress is lower in the fast cooling. Although one would expect some contribution associated with macroscopic residual stresses, they should not be higher than ±30 MPa (as shown in Table 2). The results confirm that the microscopic residual stress does not change. However, for those mixtures in which the mullite crystals are not interconnected, a significant reduction of microscopic residual stresses is observed. Those results show once again the role of mullite as a reinforcing phase, when the pieces are fast cooled. It is possible that microscopic stress reduction is related to the coalescence of cracks that ultimately reduces the efforts on quartz particles. This is consistent with the role of interconnection of mullite crystals, which would hinder the coalescence of cracks.

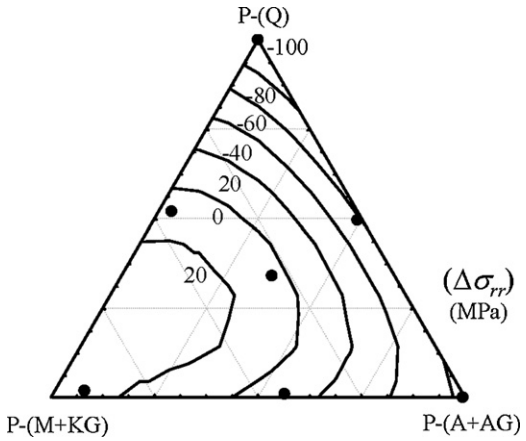

Fig. 9. Difference in microscopic residual stress on the quartz particles ($\Delta\sigma_{rr}$) between specimens produced by slow [8] and fast cooling rates.

4. Conclusions

Porcelain tile is a product that develops macroscopic residual stresses when subjected to fast cooling, as in the tempered glass. This process takes place before the allotropic transformation of quartz and may be described according to the same parameters used for glasses. Macroscopic residual stresses generally increase the mechanical strength. However, the increasing in flaw size partially reduces this effect.

When the specimens are subjected to fast cooling, such as typically in industrial process, the flaw size is the main factor determining the variation of the mechanical strength of porcelain tiles obtained from different mineralogical compositions. This increasing in natural defect size may also be interpreted from the Weibull's modulus, reaching values between 6 and 8 in those mixtures where a further deterioration of mechanical properties is detected.

The hypothesis of interconnection of mullite crystals as a mechanism for strengthening triaxial porcelain is clearly observed, but only when the specimens are fast cooled. This mechanism is the responsible for the strengthening of the microstructure by reducing the increasing of flaw size. The microscopic residual stresses by compression, caused by thermal expansion coefficients mismatch of the phases, especially from quartz particles, also act as a reinforcement mechanism.

In order to improve the mechanical strength of industrial compositions of porcelain tiles, it is necessary to increase the amount of kaolinite to starting values between 25 and 35%. The sintering temperature will probably increase, so that the amount of feldspar and/or eutectic-forming phases should also be increased. Quartz should be maintained at low level, less than 25%, and the quartz particle size must be <45 μm.

Acknowledgments

The authors wish to thank the staff at the Instituto de Tecnología Cerámica (ITC), Spain; the Coordination for the Improvement of Higher Education Personnel (CAPES), Brazil; and the Instituto Maximiliano Gaidzinski (IMG), Brazil. The authors also thank the Spanish Ministry of Industry, Tourism, and Trade for co-financing the Technology Institute Support Programme (FIT-030000-2005-315/FIT-030000-2006-119).

References

[1] T. Manfredini, G.C. Pellacani, M. Romagnoli, Am. Ceram. Soc. Bull. 74 (1995) 76–79.
[2] E. Sánchez, M.J. Orts, J.G. Ten, V. Cantavella, Am. Ceram. Soc. Bull. 80 (2001) 43–49.
[3] A. De Noni Jr., D. Hotza, V. Cantavella, E. Sanchez, Bol. Soc. Esp. Ceram. V. 46 (2007) 163–170.
[4] A. De Noni Jr., D. Hotza, V. Cantavella, E. Sanchez, J. Eur. Ceram. Soc. 28 (2008) 2463–2469.
[5] J.M. Navarro, F. El Vidrio, Constitución, Fabricación y Propiedades, 3rd ed., CSIC, Madrid, 2003.
[6] A. De Noni Jr., D. Hotza, V. Cantavella, E. Sanchez, J. Eur. Ceram. Soc. 28 (2008) 2629–2637.
[7] V.M. Slavo, L. Larentis, D.J. Green, J. Am. Ceram. Soc. 84 (2001) 1827–1831.
[8] A. De Noni Jr., D. Hotza, V. Cantavella, E. Sanchez, Mater. Sci. Eng. A 527 (2010) 1730–1735.
[9] A. De Noni Jr., D. Hotza, V. Cantavella, E. Sanchez, Mater. Sci. Eng. A 527 (2010) 1736–1743.
[10] J. Lu, Handbook of Measurement of Residual Stress, Society for Experimental Mechanics, Fairmont Press, Lilburn, USA, 1996.
[11] R. Torrecillas, J.S. Moya, Bol. Soc. Esp. Ceram. V. 27 (1988) 123–134.
[12] A. De Noni Jr., D. Hotza, V. Cantavella, E. Sanchez, J. Eur. Ceram. Soc. 29 (2009) 1039–1046.